Current Biology, Volume *30*

Supplemental Information

Synaptic Protein Degradation Controls Sexually Dimorphic Circuits through Regulation of DCC/UNC-40

Yehuda Salzberg, Vladyslava Pechuk, Asaf Gat, Hagar Setty, Sapir Sela, and Meital Oren-Suissa

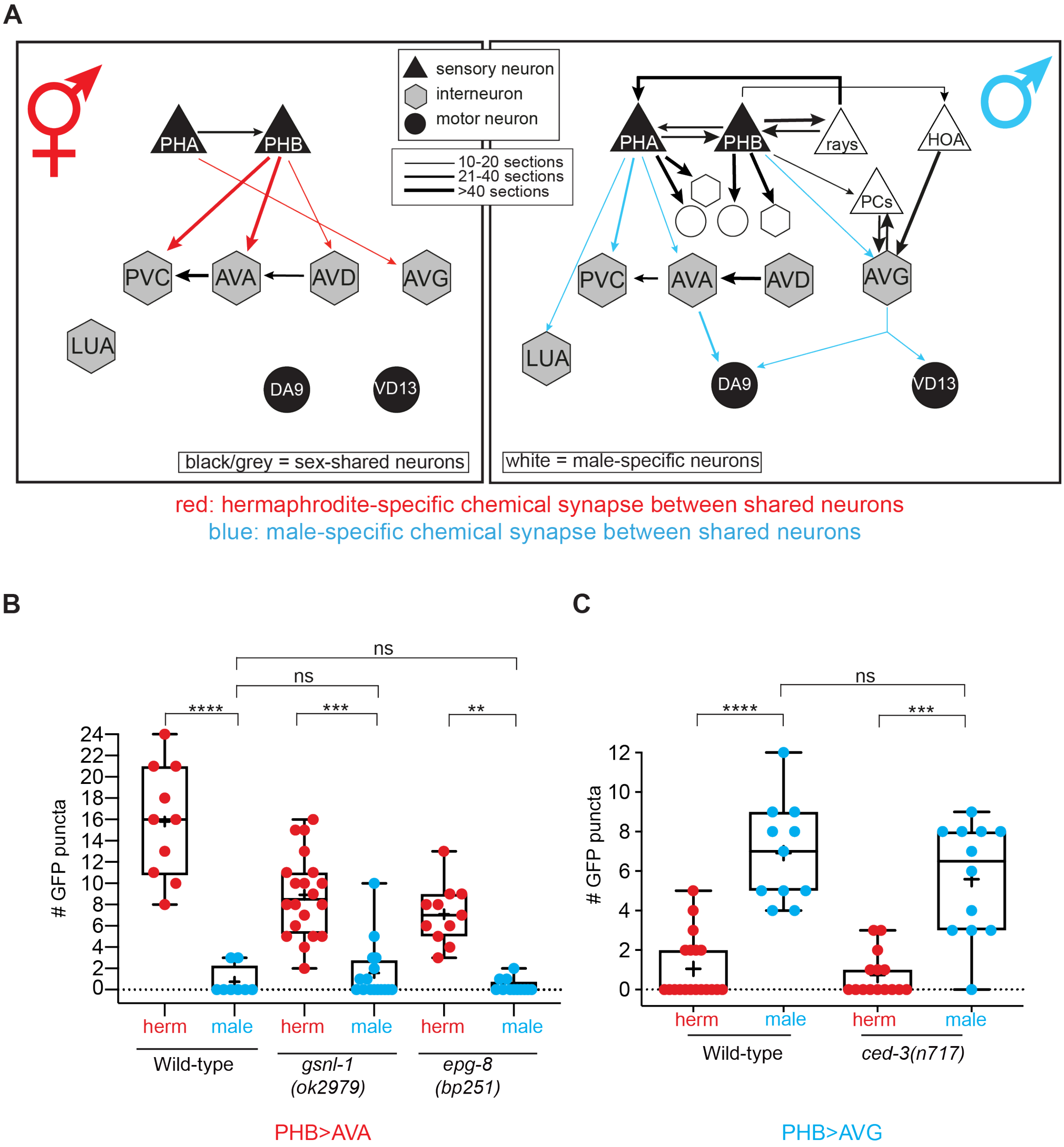

Figure S1. Connectivity of selected neurons at the adult stage, and pathways found to be dispensable for sex-specific synapse elimination. Related to Figure 1.

(A) Inferred from serial section reconstructions of electron micrographs (www.wormwiring.org) [S1-S3]. Chemical synapses between sensory (triangles), inter- (hexagons) and motor (circles) neurons are depicted as arrows. Thickness of arrows correlates with degree of connectivity (number of sections over which en passant synapses are observed).

Quantification of synaptic puncta of (B) PHB–AVA GRASP in the background of *gsnl-1(ok2979)* and *epg-8(bp251)* mutant hermaphrodites and males, (C) PHB–AVG GRASP in the background of *ced-3(n717)* mutant hermaphrodites and males. GSNL-1/gelsolin was shown to be regulated by the caspase CED-3, which cleaves GSNL-1 and enables its actin-filament-severing activity required for selective synapse elimination [S4]. EPG-8/Atg14 is part of the autophagy nucleation complex and was shown to affect synaptic vesicle clustering [S5]. We performed Kruskal–Wallis test with Dunn's multiple comparison test. ****P < 0.0001, ***P < 0.001, **P < 0.01, NS; non-significant.

In B wild-type herm n=10; males n=8, *gsnl-1* herm n=20; males n=16, *epg-8* herm n=11; males n=12. In C wild-type herm n=19; males n=11, *ced-3* herm n=15; males n=12.

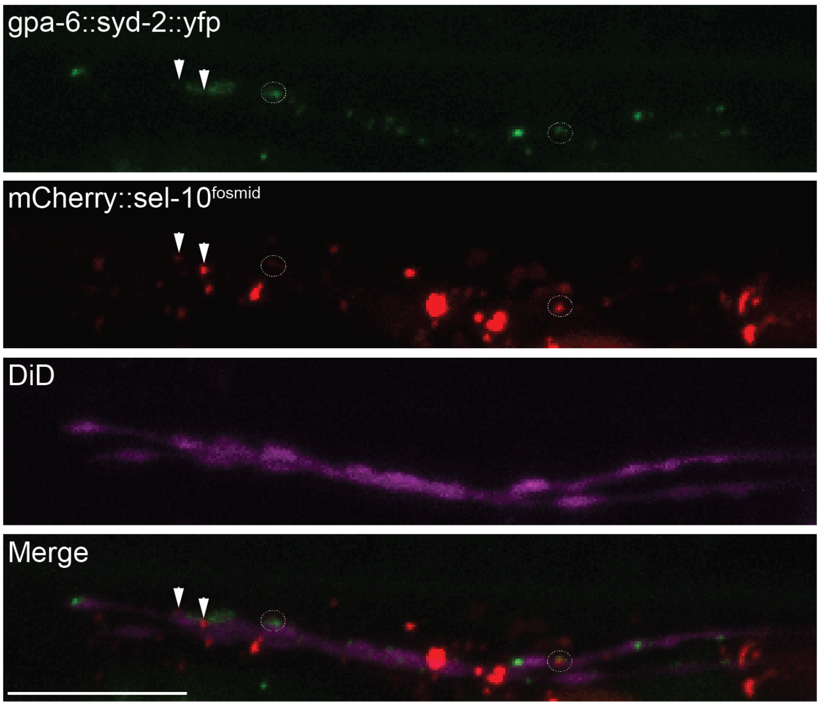

Figure S2. Some SEL-10 puncta co-localize with PHB synapses. Related to Figure 2.
Localization of mCherry::sel-10 puncta in PHB neurite. Synaptic sites are labeled with syd-2::yfp (green in figure), and Phasmids (PHA and PHB) are Dye stained (DiD, magenta in figure). Some SEL-10 puncta (Red) colocalize with SYD-2 (dashed circles, n=20 animals) and some SEL-10 puncta are found in close proximity to the YFP synaptic puncta (arrowheads). We note that PHB makes many connections with additional cells in the pre anal ganglion (Figure S1A).

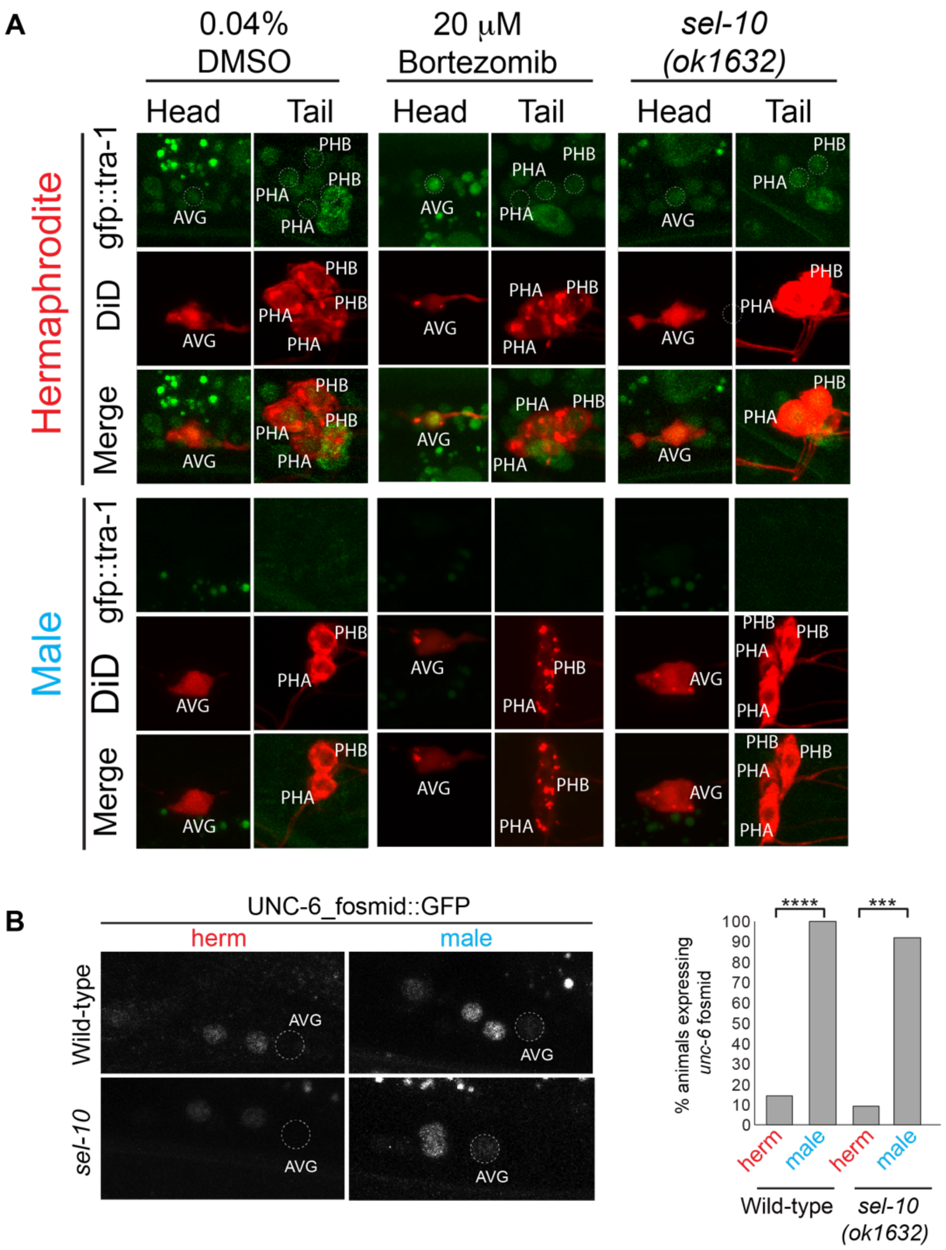

Figure S3. *sel-10* deletion animals do not show masculinization phenotypes. Related to Figures 2 and 3.

(A) Fluorescent micrographs of animals with a gfp-tagged *tra-1* locus (*tra-1(ez72)*), treated with Bortezomib or crossed to *sel-10* loss of function mutants. To identify AVG neurons an AVG::mCherry transgene was used, and to label the sensory phasmid neurons animals were stained with the lipophilic stain DiD. TRA-1 levels stay on in hermaphrodites and off in males upon inhibition of protein degradation (middle panel) and in the absence of *sel-10* (right panel), compared with controls (left panel). At least 15 animals were scored for each background. The *sel-10* allele analyzed here is a predicted null. Previously reported sexual phenotypes were based on a mis-sense change of function mutation in the WD repeat domain [S6].

(B) *unc-6* expression is unaffected in *sel-10* mutants and remains dimorphic. *unc-6* levels are measured using a fosmid reporter (*otIs638*). Statistics were calculated using Fischer's Exact test. ****$P < 0.0001$, ***$P < 0.001$.Wild-type hermaphrodites n=14; males n=11, *sel-10* herm n=11; males n=12.

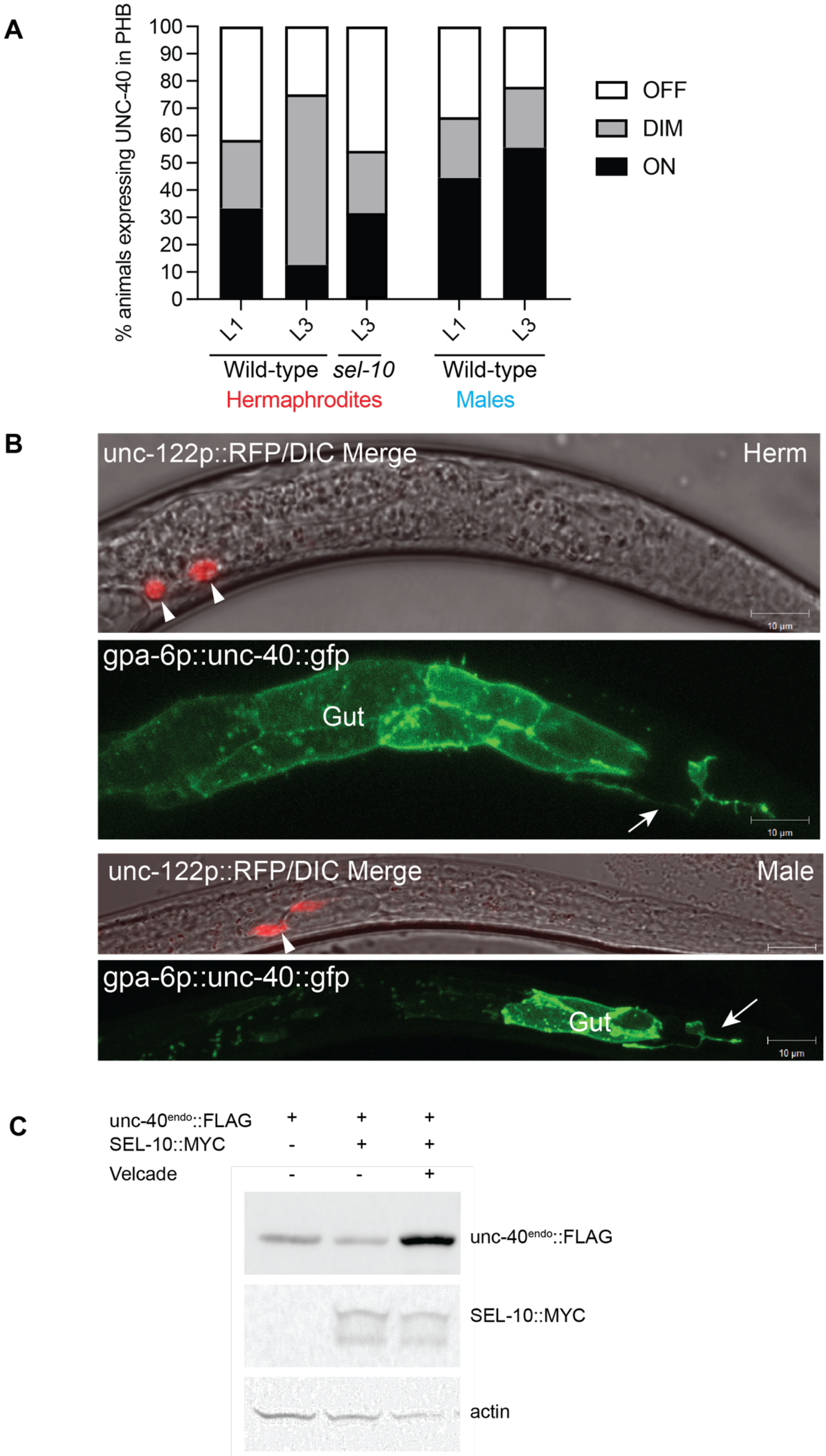
A
% animals expressing UNC-40 in PHB
100
90
80
70
60
50
40
30
20
10
0
OFF
DIM
ON
L1
L3
L3
L1
L3
Wild-type
sel-10
Wild-type
Hermaphrodites
Males
B
unc-122p::RFP/DIC Merge
Herm
gpa-6p::unc-40::gfp
Gut
unc-122p::RFP/DIC Merge
Male
gpa-6p::unc-40::gfp
Gut
C
unc-40endo::FLAG
SEL-10::MYC
Velcade
unc-40endo::FLAG
SEL-10::MYC
actin

Figure S4. Developmental analysis of UNC-40 expression levels in PHBs. Related to Figure 4.

(A) Quantification of fluorescence intensity in both sexes at L1 and L3 developmental stages, binned as high expression (on), low expression (dim) or no expression (off). Hermaphrodites: L1 n=12; L3 n=8, *sel-10* L3 n=13, Males: L1 n=9; L3 n=9. (See Figure 4A).

(B) Fluorescence micrographs of UNC-40::GFP expression in hermaphrodites of the designated genotypes and developmental time points (arrows). Expression was driven by a PHB-specific promoter in a multi-copy array. Scale bars represent 10 μm. To distinguish between the sexes at the L1 stage, coelomocyte position (arrowheads) with respect to the gonadal primordium was imaged and scored [S7, S8]. (See Figure 4A).

(C) Inhibiting the UPS suppresses sel-10-mediated degradation of UNC-40/DCC. Western blot on transfected HEK293t cells, showing that SEL-10 mediated degradation of an UNC-40 intracellular fragment (UNC-40^{endo}, residues 1108-1415) is blocked upon addition of the proteasome inhibitor velcade (10 μM for 16 hours). SEL-10 was tagged with a myc tag and UNC-40^{endo} with a FLAG tag. (See Figure 4E).

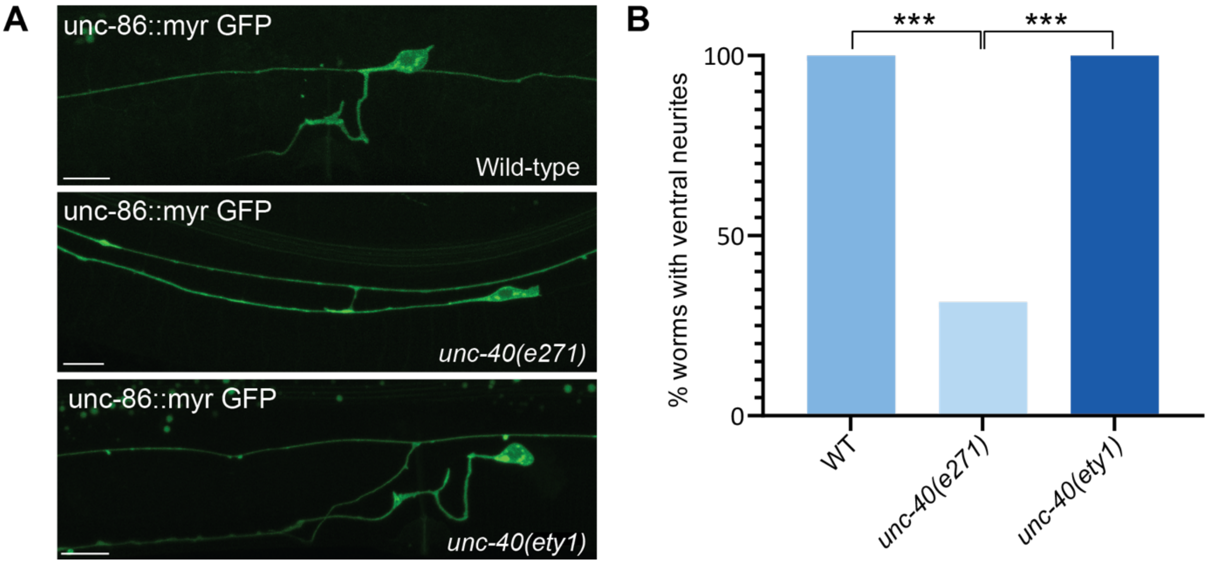

Figure S5. CPD-mutated *unc-40* animals do not show guidance defects in HSN neurite. Related to Figure 5.

(A) Fluorescence micrographs of unc-86::myr::GFP in wild type, *unc-40*(*e271) a*nd *unc-40*(*ety1)* CPD mutant animals. Scale bars represent 10 µm.

(B) Percentage of animals with ventral HSN neurites in wild-type, *unc-40(e271)* and *unc-40* CPD mutant (*ety1*) animals. Wile-type n = 20; *unc-40 (e271*) n = 19; *unc-40(ety1)* n = 30.

In panel B we performed Fisher's exact test followed by Benferroni correction for multiple comparisons. ****P* < 0.001.

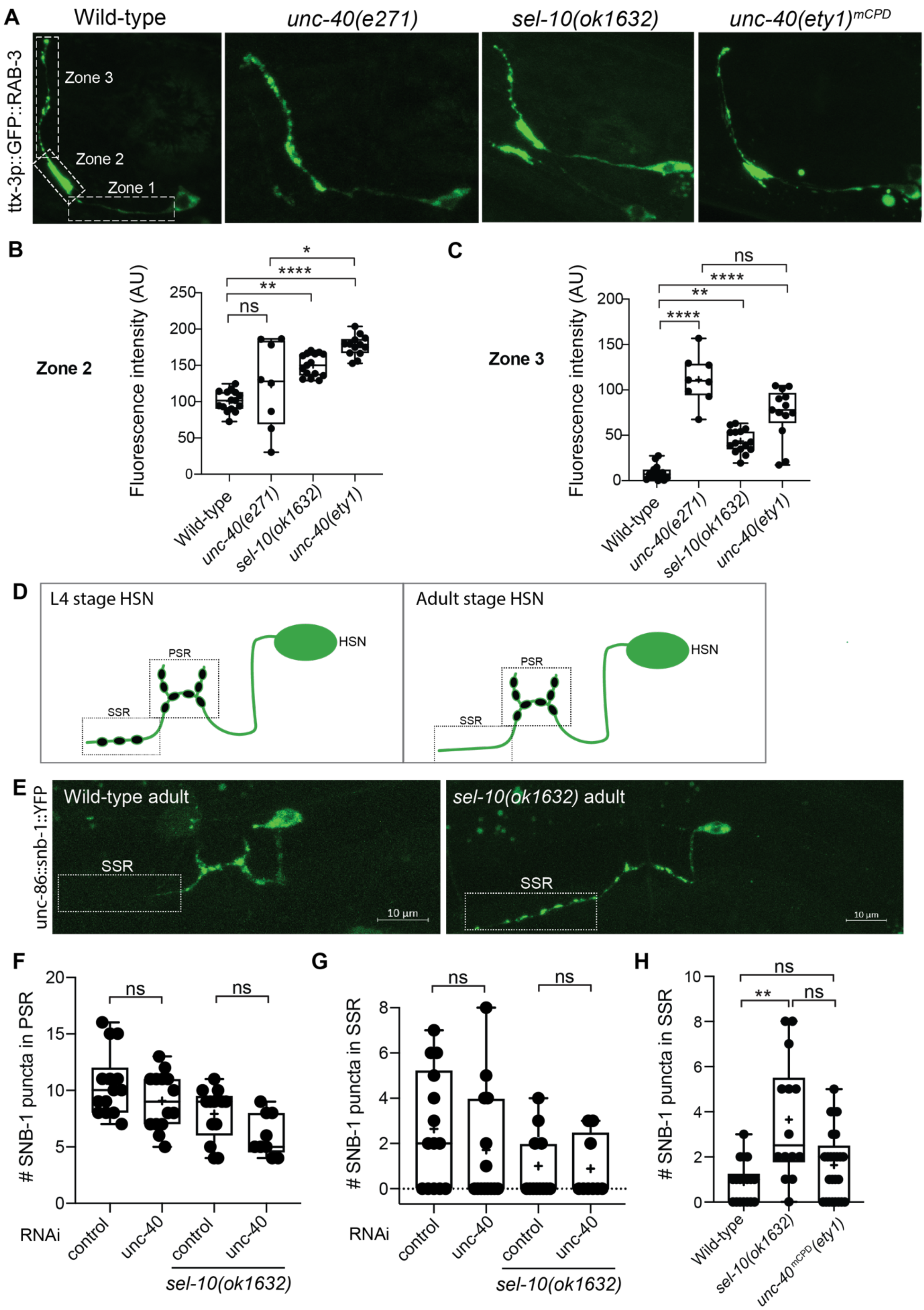

A
Wild-type
unc-40(e271)
sel-10(ok1632)
unc-40(ety1)mCPD
ttx-3p::GFP::RAB-3
Zone 3
Zone 2
Zone 1
B
Zone 2
Fluorescence intensity (AU)
Wild-type
unc-40(e271)
sel-10(ok1632)
unc-40(ety1)
C
Zone 3
Fluorescence intensity (AU)
D
L4 stage HSN
Adult stage HSN
HSN
PSR
SSR
E
unc-86::snb-1::YFP
Wild-type adult
sel-10(ok1632) adult
SSR
10 µm
F
SNB-1 puncta in PSR
RNAi
control
unc-40
sel-10(ok1632)
G
SNB-1 puncta in SSR
H
SNB-1 puncta in SSR
Wild-type
sel-10(ok1632)
unc-40mCPD(ety1)

Figure S6. Interaction between *sel-10* and *unc-40* in other synaptic contexts. Related to Figure 3.

(A) Distribution of presynaptic sites of AIY in wild-type**,** *unc-40*(*e271), sel-10(ok1632)* and *unc-40*(*ety1)* CPD mutant animals. Confocal fluorescent micrographs of GFP::RAB-3 demonstrate the distribution pattern of presynaptic vesicles in AIY. Electron microscopy reconstructions have shown that AIY has three anatomical distinct regions along its process; zone 1 has no synapses, the dorsal turn of AIY (zone 2) and the distal axon segment within the nerve ring [S9, S10]. Diagrams below micrographs depict the three different zones in the different genetic backgrounds.

(B-C) Quantification of the fluorescence intensity (arbitrary units, AU) of synaptic vesicles in zone 2 (B) and zone 3 (C). Wild-type n=15, *unc-40(e271)* n=8, *sel-10(ok1632)* n=15, *unc-40 (ety1)* n=13.

(D) Schematic of HSN neuron and its synapses in L4 and adult stages [S11]. Shown in the scheme are synapses of the primary synaptic region (PSR, dashed square) and the secondary synaptic region (SSR, dashed rectangle).D

(E) Fluorescence micrographs of SNB-1::YFP in WT animals and in *sel-10(ok1632*) mutants. SSR is shown in dashed rectangle. Scale bars represent 10 μm.

(F-G) Quantification of SNB-1::YFP synaptic puncta in the PSR (C) and in the SSR (D) in animals fed control empty RNAi plasmid or RNAi plasmid targeting *unc-40*, in a wild type or *sel-10(ok1632)* mutant backgrounds. Wild type ctrl n=14; *unc-40* RNAi n=14, *sel-10* ctrl n = 13; *unc-40* RNAi n=9.

(H) Quantification of SNB-1::YFP synaptic puncta in the SSR in wild type, *sel-10*(*ok1632)* mutants and *unc-40*(*ety1)* CPD mutants. Wild type n=18; *sel-10* n=14; *unc-40* CPD n=25.

In B, C, H we performed Kruskal–Wallis test followed by Dunn's multiple comparison test.

In F-G we performed One-way ANOVA test followed by Sidak's multiple comparison test. In panel E we performed Kruskal–Wallis test followed by Dunn's multiple comparison test. ****P < 0.0001, **P < 0.01, *P < 0.05, NS; non-significant.

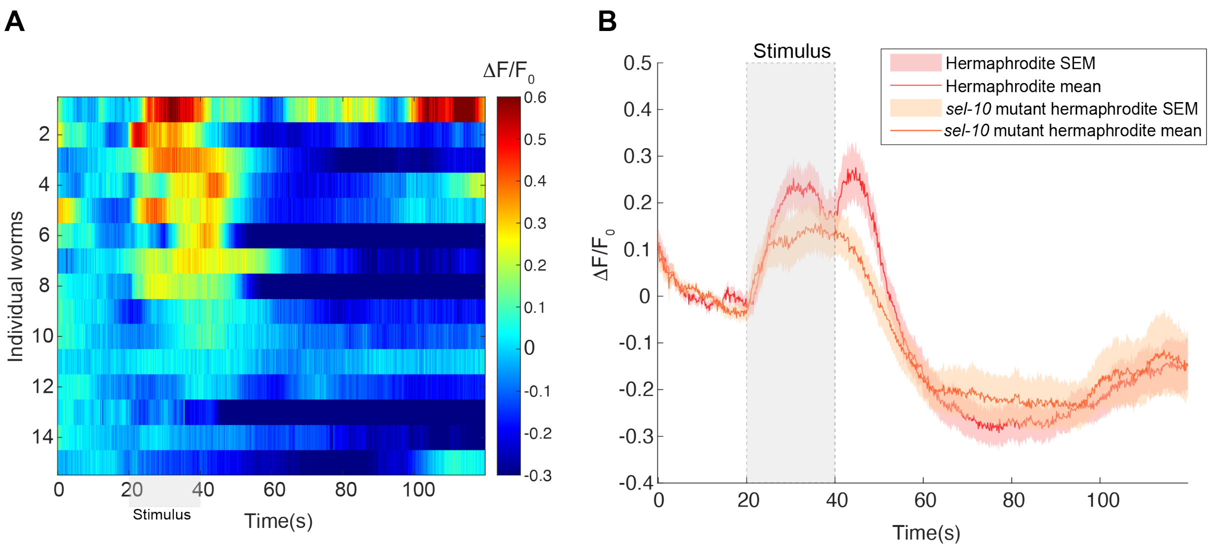

Figure S7. *Sel-10* loss of function attenuates the hermaphrodite response to glycerol. Related to Figure 6.

(A) Individual worms' AVG calcium traces of *sel-10* mutant hermaphrodites in response to 2 M glycerol. Normalized GCaMP6s signal ΔF/F0 is color-coded (Color bar shows color range according to normalized fluorescence intensities). Stimulus was delivered at 20 to 40 sec, total imaging duration was 2 min.

(B) Average GCaMP6s signals of AVG neurons of wild-type hermaphrodites (red), and *sel-10* mutant hermaphrodites (orange) in response to the stimulus. The colored lines and shaded area surrounding them indicate the mean values of ΔF/F0 and SEM, respectively.

identifier	sequence	purpose
GRASPbb_F1u	GAATTCCAACTGAGCGCCGGTCG	Gibson cloning of *sel-10* cDNA under PHB or AVG promoter (*sel-10* sequence in red)
GRASPbb _R1u	GCTAGCCAAGGGTCCTCCTGAA	
sel10_F1	TTCAGGAGGACCCTTGGCTAGC ATGTGGCCACGAAATGATGTAC	
sel10_R1	CGACCGGCGCTCAGTTGGAATTC TTAAGGGTATACAGCATCAAAGTCG	
pCDNA3.1 R1u	GGATCCGAGCTCGGTACCAAGC	Gibson cloning of UNC-40^{endodomain} into pcDNA3.1
pCDNA3.1 F1u	GAATTCTGCAGATATCCAGCACAGTGGC	
unc-40dNtFLAG F1	GCTTGGTACCGAGCTCGGATCC ATGCATCAAGTCAGCAATTTACTTC	
unc-40dNtFLAG R1	GCCACTGTGCTGGATATCTGCAGAATTC TTACCTTCGAACCGAGGG	
dpy-10 crRNA	GCUACCAUAGGCACCACGAGGUUUUAG AGCUAUGCUGUUUUG (dpy-10 sequence in red)	Co-CRISPR for unc-40 CPD mutagenesis (with dpy-10 as marker, see Paix et al, 2015 [S12])
unc-40 CPD1 crRNA	GCAUUUGCAGCUGAUGAAUUGUUUUA GAGCUAUGCUGUUUUG (unc-40 sequence in red)	
dpy-10 ssODN	CACTTGAACTTCAATACGGCAAGATGAGAATGACTGG AAACCGTACCGCATGCGGTGCCTATGGTAGCGGAGCT TCACATGGCTTCAGACCAACAGCCTAT	
unc-40 ssODN	CCTACAGTAATCGATGGATACCGTACTCTACGTGGAG CACCCCCGAATGCATCAGCTGCAAATGCTCTTCGGTC ATTCACTCAATTGG (CPD mutations in red, silent mutations for PAM erasure and restriction site in yellow)	
CPDm_val_f1	GGCATCAGGTTGGAGTCATT	Genotyping of unc-40^{mCPD} crispr allele
CPDm_val_r1	TCTCTCCATTCGATGAACCA	
CPDm_val_f2	CTACGTGGAGCACCCCCGAATG	
MVC6-CPD-F	GGAaCACCtCCaAATtCATCAGCTGCATA AGAATTCCAACTGAGCGCCGGTCG	Cloning of UNC-40 CPD peptide (12aa) under PHB promoter using site directed mutagenesis
MVC6-CPD-R	AGCTGATGaATTtGGaGGTGtTCCACGTA GCATGCTAGCCAAGGGTCCTCCTG	
RH-inx-18b A	TATGTGATAAGAAGTTCTGAGAAG	PCR fusion to generate inx-18b::GCaMP6s fragment
Inx-18b R1	CTTCTACTTGAATCAACCATTTCTACCG GTACCGTCGACG	
GCaMP6s F1	ATGGTTGATTCAAGTAGAAG	
GCaMP6s R1	CCGTACGGCCGACTAGTAGGAA	
RH-inx-18b A-nes	TTCTCTACTTTTTTCAGCGGG	
GCaMP6s nested R1	GAAACAGTTATGTTTGGTATATTGG	

Table S1. List of DNA and RNA oligonucleotides used in this study. Related to STAR Methods.

Figure 1C	PHB>AVA males n=17 DMSO treated; n=16 Bortezomib treated, PHB>AVG hermaphrodites n=13 DMSO treated; n=17 Bortezomib treated, PHA>AVG males n=11 DMSO treated; n=11 Bortezomib treated
Figure 1E	*uba-1* 15°C n=16, *uba-1* 25°C L3 shifted n=12, *uba-1* 25°C L1 shifted n=16, *uba-1* 25°C PHB-UBA-1 rescue n=15, *uba-1* 25°C AVG-UBA-1 rescue n=14, wild-type males n=14, *uba-1* 25°C L1 shifted males n=10
Figure 2A	Wild-type herm n=11; males n=11, *sel-10(ok1632)* herm n=15; males n=12, *sel-10* PHB rescue herm n=16, *sel-10* AVG rescue herm n=16
Figure 2B	Herm n=17, males n=10, herm expressing AVG::UNC-6 n=8
Figure 2C	Control herm n=12; males n=12, *skr-1* herm n=16; males n=13
Figure 2D	Herm n=13; males n=21, *sel-10(ok1632)* herm n=15; males n=15
Figure 3C	Wild-type herm n=11; males n=11, *unc-40(e271)* herm n=11; males n=16, *sel-10;unc-40* herm n=14; males n=8
Figure 3D	Wild-type herm n=11; males n=11, *sel-10(ok1632)* herm n=17; males n=11, *unc-6(ev400)* herm n=16; males n=10, *sel-10;unc-6* herm n=10; males n=13
Figure 3E	*unc-6* DMSO n=17, *unc-6* with Bortezomib n=22
Figure 3G	DMSO treated herm n=12, Sulfopin fed herm n=15, *pinn-1(tm2235)* herm n=15, *unc-40* n=15, *unc-40; pinn-1* n=16
Figure 3I	DMSO treated herm n=19, GSK-3 treated animals n=19, *unc-40* DMSO n=12, *unc-40* treated with inhibitor n=16
Figure 4A	Hermaphrodites: Wild-type L4 n=15; adult n=12; *sel-10* L4 n=10; adult n=12, Males: Wild-type L4 n=10; adult n=11; *sel-10* L4 n=9; adult n=10; *unc-6* L4 n=10; adult n=14
Figure 4D	Wild-type herm n=19; males n=12, *unc-40(ety1)* herm n=20; males n=25, *unc-6(ev400)* herm n=14; males n=12, *unc-6:unc-40* mCPD herm n=14; males n=8
Figure 4F	Control n=16, CPD peptide n=8
Figure 5A-C	n=20 animals per group
Figure 5D	Wild-type herm n=25; males n=23, *unc-40 CPD* herm n=28; males n=27, *unc-40(e271)* herm n=23; males n=12
Figure 6B-D	n = 15 per each group

Table S2. Reporting on number of animals used in each experiment. Related to STAR Methods.

Supplemental references

S1. White, J. G., Southgate, E., Thomson, J. N., and Brenner, S. (1986). The structure of the nervous system of *Caenorhabditis elegans*. Philos. Trans. R. Soc. Lond. B Biol. Sci *314*, 1–340.

S2. Jarrell, T. A., Wang, Y., Bloniarz, A. E., Brittin, C. A., Xu, M., Thomson, J. N., Albertson, D. G., Hall, D. H., and Emmons, S. W. (2012). The connectome of a decision-making neural network. Science *337*, 437–444.

S3. Cook, S. J., Jarrell, T. A., Brittin, C. A., Wang, Y., Bloniarz, A. E., Yakovlev, M. A., Nguyen, K. C. Q., Tang, L. T.-H., Bayer, E. A., Duerr, J. S., et al. (2019). Whole-animal connectomes of both *Caenorhabditis elegans* sexes. Nature *571*, 63–71.

S4. Meng, L., Mulcahy, B., Cook, S. J., Neubauer, M., Wan, A., Jin, Y., and Yan, D. (2015). The Cell Death Pathway Regulates Synapse Elimination through Cleavage of Gelsolin in *Caenorhabditis elegans* Neurons. Cell Rep *11*, 1737–1748.

S5. Stavoe, A. K., Hill, S. E., Hall, D. H., and Colon-Ramos, D. A. (2016). KIF1A/UNC-104 Transports ATG-9 to Regulate Neurodevelopment and Autophagy at Synapses. Dev Cell *38*, 171–185.

S6. Jäger, S., Schwartz, H. T., Horvitz, H. R., and Conradt, B. (2004). The *Caenorhabditis elegans* F-box protein SEL-10 promotes female development and may target FEM-1 and FEM-3 for degradation by the proteasome. Proc Natl Acad Sci USA *101*, 12549–12554.

S7. Sulston, J. E., and Horvitz, H. R. (1977). Postembryonic cell lineages of the nematode *Caenorhabditis elegans*. Dev. Biol. *56*, 110–156.

S8. Sulston, J. E., and White, J. G. (1980). Regulation and cell autonomy during postembryonic development of *Caenorhabditis elegans*. Dev. Biol. *78*, 577–597.

S9. White, J. G., Southgate, E., Thomson, J. N., and Brenner, S. (1983). Factors that determine connectivity in the nervous system of *Caenorhabditis elegans*. Cold Spring Harbor Symp. Quant. Biol. *48*, 633–640.

S10. Colón-Ramos, D. A., Margeta, M. A., and Shen, K. (2007). Glia promote local synaptogenesis through UNC-6 (netrin) signaling in *C. elegans*. Science *318*, 103–106.

S11. Wanner, N., Noutsou, F., Baumeister, R., Walz, G., Huber, T. B., and Neumann-Haefelin, E. (2011). Functional and spatial analysis of *C. elegans* SYG-1 and SYG-2, orthologs of the Neph/nephrin cell adhesion module directing selective synaptogenesis. PLoS ONE *6*, e23598.

S12. Paix, A., Folkmann, A., Rasoloson, D., and Seydoux, G. (2015). High Efficiency, Homology-Directed Genome Editing in *Caenorhabditis elegans* Using CRISPR-Cas9 Ribonucleoprotein Complexes. Genetics *201*, 47–54.